Sensitivity of Ocean Surface Salinity Measurements From Spaceborne L-Band Radiometers to Ancillary Sea Surface Temperature

Thomas Meissner, *Senior Member, IEEE*, Frank J. Wentz, Joel Scott, and Jorge Vazquez-Cuervo

***Abstract*—Sea surface temperature (SST) serves as a crucial ancillary input field to the retrieval algorithm for sea surface salinity (SSS) from L-band satellite radiometers, such as Soil Moisture and Ocean Salinity mission, Aquarius, and Soil Moisture Active Passive mission. It is needed for inverting the radiative transfer model equation of the ocean surface emissivity, which depends both on ocean surface salinity and ocean surface temperature. Our analysis studies the sensitivity of the performance of the Aquarius salinity retrieval algorithm to the ancillary SST that is used in the algorithm. We have retrieved Aquarius salinities using four different SST fields as ancillary input, namely, the National Oceanic and Atmospheric Administration (NOAA) Advanced Very High Resolution Radiometer (AVHRR)-only Optimum Interpolation SST (OISST), the SST from WindSat, the SST from the Canadian Meteorological Center (CMC), and the Multi-scale Ultra-high Resolution (MUR) SST from the National Aeronautics and Space Administration's Jet Propulsion Laboratory. The retrieved Aquarius SSS is compared with ground truth data; thus, the performance of the salinity retrieval algorithm in all four cases can be evaluated. The WindSat, CMC, and MUR SST products, which are all based on or are assimilating SST measurements from the passive microwave (MW) sensors, give better performance than the NOAA AVHRR-only OISST, which does not use any MW SST data, but which is solely based on the *in situ* data and observations from the infrared AVHRR sensor. The CMC SST gives the best overall performance for the retrieved SSS. The sensitivity of the SSS retrievals and therefore the performance differences between the various ancillary input fields increases in cold water.**

***Index Terms*—Enter L-band, microwave radiometry, ocean salinity, ocean temperature, passive microwave remote sensing.**

I. Introduction

THE Aquarius/SAC-D L-band radiometer/scatterometer system has been designed to provide sea surface salinity (SSS) salinity maps at a 150-km spatial scale at an accuracy of 0.2 psu [1] over monthly averages. The instrument provided science data starting August 25, 2011 before the observatory suffered a mission-ending hardware failure on June 7, 2015. This leaves a legacy data set of SSS measurements of more than 45 months. The SSS retrieval algorithm has undergone numerous improvements and refinements [2]–[7]. The most recent Version 4.0 [5] has been released on July 17, 2015, and it has been validated that it fulfills the primary mission accuracy requirement of 0.2 psu [8].

The SSS retrieval algorithm takes Aquarius antenna temperatures (T_A) as input and transforms them into brightness temperatures T_{B0} for a flat ocean surface. In this process, a series of spurious signals need to be removed step by step: 1) cosmic, galactic, solar, and lunar radiation; 2) antenna cross polarization; 3) radiation from land surfaces near ocean–land boundaries; 4) Faraday rotation in the Earth ionosphere; 5) atmospheric attenuation by oxygen, water vapor, and liquid cloud water; and 6) effects from the wind-roughened ocean surface. The Aquarius measurements are also filtered for radio-frequency interference (RFI) [9], [10]. The final step in determining SSS is to match this measured T_{B0} at the flat ocean surface with the value that is obtained from the Fresnel equations that characterize the electromagnetic emission from a specular ocean surface based on the Meissner–Wentz model for the permittivity (dielectric constant) of sea-water [11], [12]. Because the model function for T_{B0} depends on sea surface temperature (SST), it is necessary to use an ancillary SST field as input to the SSS retrieval algorithm.

The purpose of this paper is to investigate the sensitivity of the SSS retrievals to the ancillary SST input field. We have run and evaluated the performance of the Aquarius SSS retrieval algorithm with four different SST fields as ancillary input: the National Oceanic and Atmospheric Administration (NOAA) Advanced Very High Resolution Radiometer (AVHRR)-Optimum Interpolation SST (OISST), the weekly SST averages from WindSat, the Canadian Meteorological Center (CMC) daily SST, and the Multi-Scale Ultra-High Resolution (MUR) SST from the Jet Propulsion Laboratory (JPL). All these products are distributed through the Group for High-Resolution SST (GHRSST). The last three SST products are all based on or assimilate SST measurements from spaceborne microwave sensors, whereas the NOAA AVHRR-only OISST does not ingest any microwave SST, but rather uses infrared-derived SSTs.

Our paper is organized as follows. In Section II, we provide a simple estimate of the sensitivity of the SSS retrieval on SST. Section III gives an overview over the evaluated SST data

Manuscript received March 16, 2016; revised May 30, 2016; accepted July 21, 2016. Date of publication August 19, 2016; date of current version September 30, 2016. This work was supported by the National Aeronautics and Space Administration under Contract NNG04HZ29C.

T. Meissner and F. J. Wentz are with Remote Sensing Systems, Santa Rosa, CA 95401 USA (e-mail: meissner@remss.com; frank.wentz@remss.com).

J. Scott was with Remote Sensing Systems, Santa Rosa, CA 95401 USA. He is now with the Ocean Biology Processing Group, NASA Goddard Space Flight Center, Greenbelt, MD 20771 USA (e-mail: Joel.p.scott@gmail.com).

J. Vasquez-Cuervo is with the Jet Propulsion Laboratory, California Institute of Technology, Pasadena, CA 91109 USA (e-mail: Jorge.Vazquez@jpl.nasa.gov).

Color versions of one or more of the figures in this paper are available online at http://ieeexplore.ieee.org.

Digital Object Identifier 10.1109/TGRS.2016.2596100

sets. The results on the performance comparison of Aquarius SSS retrievals are presented in Section IV. Section V briefly summarizes our main results and conclusions.

II. Estimate of the Sensitivity of SSS Retrievals to SST

The purpose of this section is to provide a simple estimate of the sensitivity of the retrieved SSS to the ancillary SST field. This estimate is based on the physics of the electromagnetic microwave emission of a flat ocean surface at the L-band. Although the results of this section will not be used in the following data analysis, we believe that the findings are useful for demonstrating and understanding the major cause of the sensitivity of the SSS to the ancillary SST.

The crucial step, in which the ancillary SST field T enters the Aquarius SSS retrieval algorithm, is in the calculation of the brightness temperature $T_{B0,\mathrm{mod}} = E_0(T,S)\cdot T$ that is emitted by a flat ocean surface. The flat surface emissivity $E_0(T,S)$ is given by the Fresnel equations of specular reflection and is determined by the model of the dielectric constant of sea water [11], [12]. It depends both on the T (SST) and on the S (SSS). The SSS retrieval algorithm matches the model for T_{B0} to the Aquarius measurement in a maximum likelihood estimate. In addition, the specular reflection of the SST ancillary field is also used in the SSS retrieval algorithm to calculate the correction for atmospheric absorption [2] and to derive the correction for the wind-roughened surface [10], but the magnitude of these two corrections is an order of magnitude smaller compared with the size of T_{B0}. We can obtain a simple estimate of the sensitivity of the retrieved Aquarius SSS to the ancillary SST input field from the matching condition

$$T_{B0,\mathrm{meas}} = T_{B.0.\mathrm{mod}}(T,S) = E_{0,\mathrm{mod}}(T,S)\cdot T. \qquad (1)$$

If we assume that the matching is done only for the vertical polarization (v-pol), we can formally take the partial derivative of (1) with respect to T, i.e.,

$$0 = \frac{dT_{B,0,\mathrm{meas}}(\text{v-pol})}{dT} = \left(\frac{\partial T_{B,0,\mathrm{meas}}(\text{v-pol})}{\partial T}\right) + \left(\frac{\partial T_{B,0,\mathrm{meas}}(\text{v-pol})}{\partial S}\right)\cdot\frac{dS}{dT}. \qquad (2)$$

Equation (2) can be solved for the derivative dS/dT, which determines the sensitivity of the retrieved SSS to the ancillary SST, i.e.,

$$\frac{dS}{dT} = -\frac{\left(\frac{\partial T_{B,0,\mathrm{meas}}(\text{v-pol})}{\partial T}\right)}{\left(\frac{\partial T_{B,0,\mathrm{meas}}(\text{v-pol})}{\partial S}\right)}. \qquad (3)$$

In this simplified approach, dS/dT is thus given by the sensitivity ratio between the v-pol emitted T_{B0} from a specular ocean surface to SST and SSS, respectively. The sensitivities on the right-hand side of (3) are effectively determined by the functional dependence of the sea water dielectric constant on T and S [11], [12]. Their values can be numerically calculated from the expressions for the model function for the v-pol T_{B0} by perturbing the values for SST and SSS. The resulting curves

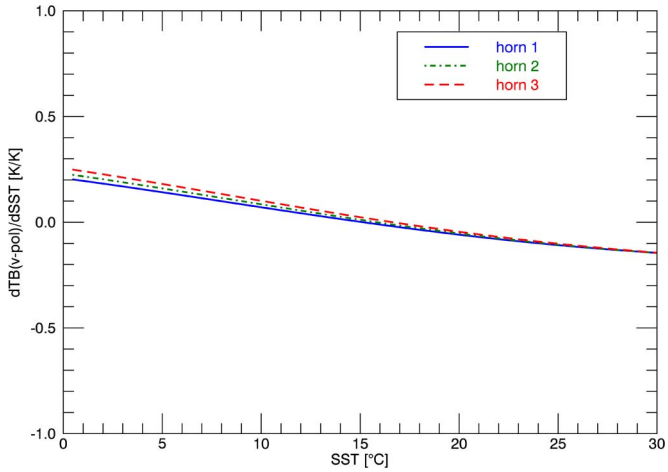

Fig. 1. Sensitivity of the v-pol brightness temperature to SST for the three Aquarius horns: solid line (horn 1), dash–dot line (horn 2), and dashed line (horn 3). In computing the curves, we set the SSS to 35 psu. The nominal values for the EIAs of the three horns are 29.36°, 38.44°, and 46.29°, respectively.

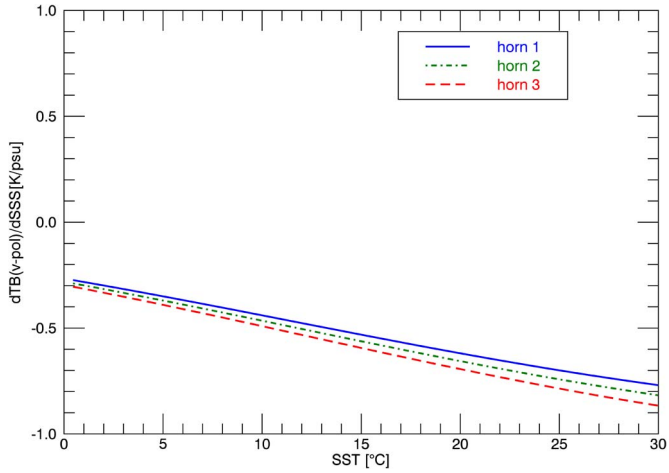

Fig. 2. Sensitivity of the v-pol brightness temperature to the SSS for the three Aquarius horns: solid line (horn 1), dash–dot line (horn 2), and dashed line (horn 3). In computing the curves, we have set the SSS to 35 psu. The nominal values for the EIAs of the three horns are 29.36°, 38.44°, and 46.29°, respectively.

for the three derivatives, namely, $\partial T_{B0}/\partial T$, $\partial T_{B0}/\partial S$, and dS/dT as a function of SST for the three Aquarius horns are shown in Figs. 1–3. As the water becomes colder, the sensitivity of T_{B0} to SST increases (see Fig. 1) and the sensitivity of T_{B0} to SSS decreases (see Fig. 2). As a consequence, the sensitivity of SSS to SST is largest in cold water (below 10 °C) and it decreases with increasing SST. For intermediate temperatures (10 °C–20 °C), the surface-emitted brightness temperature (see Fig. 1) is almost insensitive to SST. According to (3), the retrieved salinity is also insensitive to SST in the intermediate temperature range, which is evident in Fig. 3. In warm water (above 20 °C), the sensitivity of T_{B0} to SST starts increasing again, although the sign changes compared with that of cold water (see Fig. 1). At the same time, the sensitivity of T_{B0} to SSS also keeps increasing with increasing SSS (see Fig. 2). As a consequence, the sensitivity of SSS to SST starts increasing

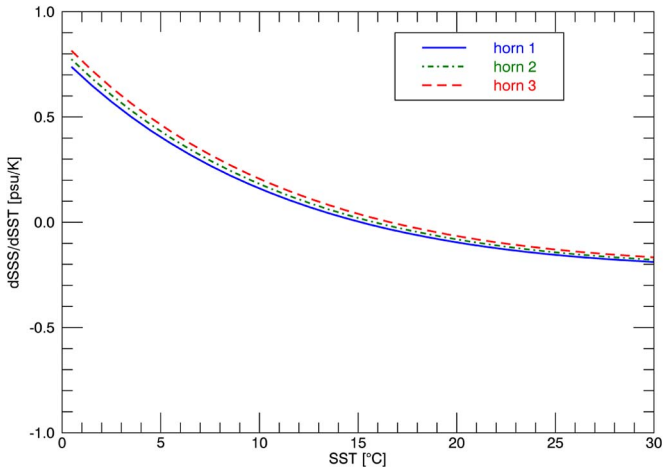

Fig. 3. Estimate of the sensitivity of the retrieved SSS to SST used as given by the derivative dS/dT in (3) as function of SST for the three Aquarius horns: solid line (horn 1), dash–dot line (horn 2), and dashed line (horn 3). In computing the curves we have set SSS to 35 psu. The nominal values for the EIAs of the three horns are 29.36°, 38.44°, and 46.29°, respectively.

slightly above 20 °C, although the absolute value is smaller than it is in cold water. The sign of the derivative in Fig. 3 also implies that an increase in the ancillary SST field will increase the retrieved SSS in cold water and decrease the retrieved SSS in warm water. We also note that the sensitivity curves in Fig. 3 are largely independent of the Earth incidence angle (EIA).

The actual Aquarius Version 4.0 SSS retrieval algorithm uses both v-pol and horizontal polarization (h-pol) and performs a maximum-likelihood estimate in determining SSS [4], [7]. The curves in Fig. 3 change very little if the h-pol, rather than the v-pol, is used in the matching (1). We can, therefore, expect that our conclusions about the sensitivity of SSS to SST also hold for the actual Aquarius Version 4.0 SSS retrievals. Most importantly, we anticipate that the differences in the ancillary SST input field will impact the SSS retrievals strongest in cold water and therefore be most visible at high latitudes.

III. Study Data Sets

A. Aquarius Data

Our analysis is based on the Version 4.0 Aquarius Official Release Level 2 SSS from NASA PO.DAAC [13]. Using the provided quality control (Q/C) flags, the data have been screened for contamination from land and sea ice if the gain weighted average of either land or sea-ice fraction within the field of view exceeds 0.1%. In addition, the observations with high galactic and high lunar radiation, and those which are likely contaminated by undetected RFI, have been also excluded. The time period of our analysis spans the entire Aquarius mission, August 25, 2011–June 7, 2015.

B. SST Data Sets

The rationale for deriving the SSS using these four different SST data sets is to demonstrate the effect on the SSS retrievals attributable to the choice of SST data used. Each of these data sets described next is exemplary in the type of input SST data used, namely, *in situ*, infrared, and/or microwave SSTs. We will address the question of which one of these data sets leads to the highest quality SSS retrieval in this paper.

1) NOAA AVHRR-OISST: The NOAA AVHRR Optimally Interpolated (AVHRR-OISST) [14]–[16] was the original data set implemented in the Aquarius retrievals because of the bias-free SST estimates with respect to *in situ* data. This data set does not include any microwave-derived SSTs. It has been used as the ancillary field SST in the algorithms used for all Aquarius data releases up to the current Version 4.0. The AVHRR-OISST product is distributed through the GHRSST project and can be downloaded through the Physical Oceanography Distributed Active Archive Center (PO.DAAC) at: https://podaac.jpl.nasa.gov/dataset/NCDC-L4LRblend-GLOB-AVHRR_OI. It combines both AVHRR infrared-derived SSTs and *in situ* SSTs using optimum interpolation (OI). The Pathfinder Version 5 product is used when available, whereas the NOAA AVHRR operational product is used as a second choice. The product is available as daily 0.25° grids. Details on the optimal interpolation technique used and the AVHRR-OI data set may be found in [15].

2) WindSat SST: WindSat provides a microwave-only SST that allows for the direct comparison between an infrared-only (AVHRR-OISST) data set and a microwave-derived SST. The major advantage of the microwave sensor is the capability to retrieve SSTs under cloudy conditions. Additionally, it provides better SSS retrievals in areas of high water-vapor content and aerosols. Our analysis uses the Remote Sensing Systems (RSS) Version 7.0.1. WindSat daily 0.25° SST fields [17]. The RSS WindSat SST retrieval algorithm uses all WindSat channels at 6.8, 10.7, 18.7, 23.8, and 37.0 GHz. The WindSat SST data have been filtered for contamination from land, sea ice, and rain. In order to obtain global coverage when using the WindSat SST as ancillary input to the Aquarius SSS retrieval algorithm, we created running 7-day averages from the daily WindSat SST files that are centered on each day. Because the local ascending node times of Aquarius and WindSat are both approximately 18:00, it is possible to find matchups between Aquarius and WindSat observations within a typical time collocation window of 60 min. However, the swath of the WindSat SST field is very narrow and, therefore, many Aquarius SSS observations get lost if we use actual WindSat swath SST matchups in the Aquarius SSS processing algorithm.

3) CMC SST: The CMC product provides a data set that includes both infrared and microwave-derived SSTs. *In situ* data are also incorporated from the International Comprehensive Ocean-Atmosphere Data Set (ICOADS) data set. Thus, this SST data set should have the advantage of incorporating all three types of SST data, namely, infrared, microwave, and *in situ*. This product is distributed through the GHRSST project and can be downloaded from the PO.DAAC web site (https://podaac.jpl.nasa.gov/dataset/CMC0.2deg-CMC-L4-GLOB-v2.0). The Level 4 SST analysis is produced daily, on an operational basis, at the CMC. This data set merges infrared SSTs available at varying points in the time series from the Along-Track Scanning Radiometer (ATSR) series of radiometers onboard ERS-1, ERS-2, and Envisat, and from the AVHRR onboard NOAA-16, 17, 18, 19 and METOP-A. The microwave SSTs are from the

Tropical Rainfall Measuring Mission microwave imager (TMI), the Advanced Microwave Scanning Radiometer onboard the Earth Observing Satellite (AMSR-E) and WindSat onboard the Coriolis satellite. *In situ* observations of SST from drifting buoys and ships from the ICOADS program are included. The CMC SST data are placed on a 0.2° grid for daily maps. Unlike the AVHRR-OI, the CMC SST data set combines both infrared (ATSR, AVHRR) and microwave (TMI, AMSR-E, WindSat) using optimal interpolation [18].

4) MUR SST: The MUR SST data set differs from the previous two data sets in some key ways. Like the CMC, it uses both infrared- and microwave-derived SSTs (AMSR-E and WindSat). *In situ* data are used as reference for the removal of biases. This MUR SST product has greater numbers of cloud-free infrared-derived SSTs because of the addition of SSTs from the Moderate Resolution Imaging Spectroradiometer onboard both the Aqua and Terra platforms. MUR SSTs are distributed as part of the GHRSST project and are available through the PO.DAAC at:https://podaac.jpl.nasa.gov/dataset/JPL-L4UHfnd-GLOB-MUR. More information on the algorithm and its implementation may be found in [19]. Briefly, the data set is produced using a series of wavelets as a basis function in an optimal interpolation. Daily maps are produced on a global 0.011° global grid in near real time with a one day lag.

C. Matchup With Aquarius Observations

The NOAA AVHRR-OI, CMC SST, and MUR SST fields are daily averages. The WindSat SST fields are weekly running averages. In all cases, the SST product data fields are linearly interpolated in space and time to the Aquarius swath observations. The temporal resolution of the SST fields that are used in our analysis does not allow for assessing if the diurnal variations in the SST ancillary field might impact the SSS retrievals. We expect this impact is small and that it does not change the main conclusions of our study. As shown in [20], the diurnal warming of the ocean surface layer is sizeable during midafternoon and at low wind speeds. The Aquarius local ascending/descending node times are at 18:00 and 6:00, respectively, and thus, the diurnal warming is small. In addition, low wind speeds predominantly occur in warmer water and, as discussed in Section II, the major impact of the ancillary SST fields is expected to occur at high latitudes, where the average wind speeds are large, and therefore, rapid mixing of the ocean surface layer occurs and wipes out any diurnal SST warming.

IV. Performance Evaluation

A. Level 2 Swath Observations

Aquarius L2 SSS are retrieved in 1.44-s intervals. In order to evaluate the performance of the SSS retrievals for the different SST ancillary input fields, we use the standard deviation σ between the SSS from Aquarius and the daily HYbrid Coordinate Ocean Model (HYCOM) upper ocean layer SSS field [21]–[24] as a metric. The HYCOM SSS is first resampled to $0.25^\circ \times 0.25^\circ$ spatial resolution and then is linearly interpolated in space and time to the Aquarius Level 2 swath observations. As we are interested in the performance relative to the NOAA AVHRR-OI-derived baseline SSS product, which is used in Version 4.0, we plot the root-mean-square (rms) differences, i.e.,

$$\Delta\sigma_i = \pm\sqrt{|\sigma_i^2(\text{Aq-HYCOM}) - \sigma_0^2(\text{Aq-HYCOM})|}. \quad (4)$$

The index $i = 1, 2, 3$ in (4) indicates the retrievals with the WindSat, CMC, and MUR ancillary SST fields, respectively. The baseline case using the NOAA AVHRR-OI is labeled as $i = 0$. The $\pm$ sign in (4) applies if the standard deviation σ_i has increased/decreased from $i = 0$, and thus, the algorithm performance has decreased/increased compared with the baseline case.

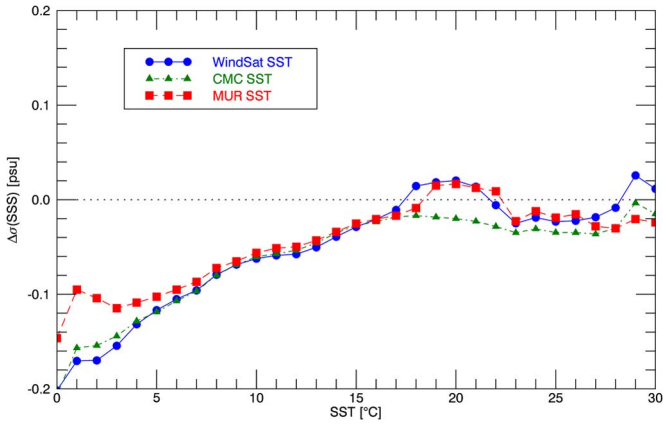

Fig. 4. Change in performance of the Aquarius L2 SSS retrievals as a function of SST used in the algorithm based on the standard deviation between Aquarius and HYCOM SSS as defined in (4). The bin size is 1 K. The circles/solid line are the results from using WindSat SST (see Section III-B2) as the ancillary SST field in the SSS retrieval, the triangles/dash–dot line are the results from using CMC SST (see Section III-B3), and the squares/dashed line are the results from using MUR SST (see Section III-B4). A positive/negative value for the performance change indicates performance degradation/improvement relative to the NOAA AVHRR-OISST product currently used for the Aquarius Version 4.0 SSS product.

Fig. 4 shows the results for $\Delta\sigma_i$ as a function of SST, where we have averaged over all three Aquarius horns. As expected from the sensitivity discussion in Section II, the SSS differences between the different ancillary SST input fields increase with a decreasing SST. It is evident that all three SST fields that use microwave satellite SST information perform better than the NOAA AVHRR-only OI baseline case. Among the three SST fields, the best overall performance is achieved when using the CMC SST. We have also checked that there are no significant biases as function of SST when retrieving Aquarius SSS using the four different SST ancillary fields $i = 0, \ldots, 3$ by comparing each of the SSS retrievals to HYCOM.

B. Monthly Averages

The Aquarius mission accuracy requirement is set for the global rms uncertainty of monthly averaged Aquarius SSS retrievals. Therefore, it is warranted to evaluate the performance between the various ancillary SST fields for the global monthly SSS averages. The rms uncertainty in the Aquarius

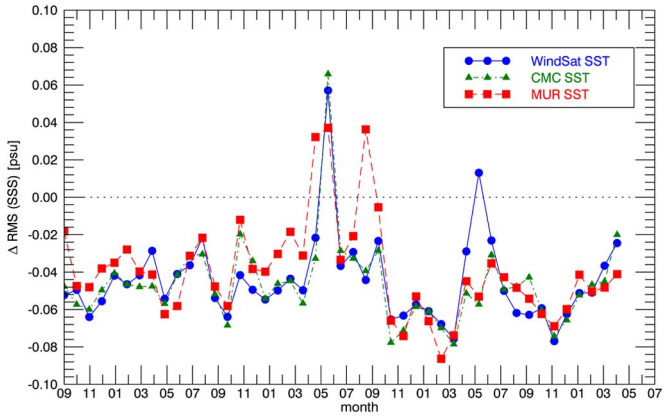

Fig. 5. Change in performance of Aquarius monthly 3° × 3° SSS averages based on the Aquarius rms error that is estimated from triple collocations between Aquarius, ARGO, and HYCOM SSS maps as defined in (6). The time period is September 2011–May 2015. The circles/solid line are the results from using WindSat SST (see Section III-B2) as the ancillary SST field in the SSS retrieval, the diamonds/dash–dot line are the results using CMC SST (see Section III-B3), and the squares/dashed line are the results using MUR SST (see Section III-B4). A positive/negative value for the performance change indicates performance degradation/improvement relative to the NOAA AVHRR-OISST field.

SSS retrievals can be estimated from the triple collocations [8] between Aquarius, ARGO [25], and HYCOM SSS values. Although the HYCOM-analyzed SSS field does assimilate information from the ARGO *in situ* measurements, it can be assumed that the errors in the ARGO and HYCOM SSS are approximately independent. On global and monthly timescales, there are no significant biases between Aquarius, ARGO, and HYCOM SSS [8]. Therefore, the individual rms uncertainties of the Aquarius, ARGO, and HYCOM SSS can be computed from the statistics for triple matchups. Specifically, the estimated rms Aquarius uncertainty is

$$\mathrm{rms}_i^2(\mathrm{Aq}) = \frac{1}{2}\left[\mathrm{rms}_i^2(\text{Aq-ARGO}) + \mathrm{rms}_i^2(\text{Aq-HYCOM}) - \mathrm{rms}_i^2(\text{Aq-HYCOM})\right]. \quad (5)$$

The index $i = 0, \ldots, 3$ runs over the different SST ancillary input fields as specified in Section IV-A. The rms of the mutual differences on the right-hand side of (5) is computed over ensembles of global monthly binned maps. As we did in the case of the individual swath observation (see Section IV-A), we consider again the performance of the three SST cases $i = 1, 2, 3$ (WindSat, CMC, MUR) relative to the baseline case $i = 0$ (NOAA AVHRR-OI) and therefore compute the following rms differences:

$$\Delta\mathrm{rms}_i = \pm\sqrt{|\mathrm{rms}_i^2(\mathrm{Aq}) - \mathrm{rms}_0^2(\mathrm{Aq})|} \quad i = 1, 2, 3. \quad (6)$$

The results for Δrms are shown in Fig. 5 as monthly time series and reveal a similar conclusion as in the case of the Level 2 swath data.

The performance estimate of the Aquarius salinity retrieval in the validation study [8] excluded observations if the SST is lower than 5 °C or if the surface wind speed exceeds 15 m/s. The reason for this is that at a very low SST, the sensitivity of the brightness temperature to the SSS gets very small (see Fig. 2) and, as a consequence, any small random or systematic uncertainties that enter the retrieval algorithm get magnified. At high wind speeds, the wind-induced emissivity signal becomes large, and thus, uncertainties in the ancillary wind speed used in the surface roughness correction [6] also grow. We have followed the same approach when calculating the performance estimate in Fig. 5 and did not include observations if the SST is lower than 5 °C or the surface wind speed exceeds 15 m/s.

TABLE I
TOTAL RMS UNCERTAINTIES OF AQUARIUS MONTHLY 3° × 3° SSS AVERAGES (IN PRACTICAL SALINITY UNITS) THAT WERE ESTIMATED FROM TRIPLE COLLOCATIONS BETWEEN AQUARIUS, ARGO AND HYCOM SSS MAPS FOR THE FOUR ANCILLARY SST FIELDS USED IN THE AQUARIUS ALGORITHM

NOAA AVHRR-OI	0.172
WindSat	0.165
CMC	0.164
MUR	0.166

During almost all months, the three SST ancillary fields tested that use microwave measurements in their production result in better performance than the NOAA AVHRR-OISST product. The differences between the three cases $i = 1, 2, 3$ are small for most months. Table I summarizes the values for the total estimated rms uncertainties in the retrieved Aquarius SSS.

V. SUMMARY AND CONCLUSION

We ran the Aquarius SSS retrieval algorithm with three different ancillary SST fields and compared the SSS values with those from the baseline SSS obtained using the NOAA AVHRR-OISST product currently used in Version 4.0 of the official data release. All of the three SST ancillary fields that were evaluated (WindSat, CMC, MUR) are based on or assimilate microwave satellite SST data. We find that all three of the SST products tested perform better in the SSS retrievals than the baseline NOAA AVHRR-OI, which only uses infrared and *in situ* SSTs but no microwave SST. SST that is retrieved from the infrared sensors is known to degrade under clouds, high water vapor (tropics), and aerosols (Saharan dust storms), whereas the microwave SST is little or not affected in these conditions. Although the infrared sensors can measure SST at much higher spatial resolutions than microwave sensors, this hardly constitutes an advantage for SSS retrievals with L-band radiometers, which have large footprint sizes of typically 40–150 km.

We obtain the best overall performance in the Level 2 product when using the CMC SSTs as the ancillary input to the Aquarius SSS retrieval algorithm. Future plans are to change the ancillary SST field used as the input to the algorithm from the NOAA AVHRR-OI to the CMC SST in the upcoming Aquarius SSS releases.

Although our analysis was completed using Aquarius SSS, we expect that the same conclusions will hold for the SSS measurements from the other L-band sensors, such as SMOS [26] or SMAP [27], [28].

ACKNOWLEDGMENT

The authors would like to thank members of the Aquarius cal/val and science teams, in particular T. Lee, for numerous useful discussions.

REFERENCES

[1] G. Lagerloef *et al.*, "The Aquarius/SAC-D mission: Designed to meet the salinity remote-sensing challenge," *Oceanography*, vol. 21, no. 1, pp. 68–81, Mar. 2008. [Online]. Available: 10.5670/oceanog.2008.68

[2] F. Wentz and D. Le Vine, *Aquarius Salinity Retrieval Algorithm Theoretical Basis Document (ATBD)*. Santa Rosa, CA, USA: Remote Sens. Syst., Aug. 2012. [Online]. Available: http://podaac.jpl.nasa.gov/SeaSurfaceSalinity/Aquarius

[3] D. Le Vine, T. Meissner, F. Wentz, and J. Piepmeier, *Aquarius Salinity Retrieval Algorithm Theoretical Basis Document (ATBD), Addendum 2*. Santa Rosa, CA, USA: Remote Sens. Syst., Aug. 2012. [Online]. Available: http://podaac.jpl.nasa.gov/SeaSurfaceSalinity/Aquarius

[4] T. Meissner, F. Wentz, D. Le Vine, and J. Scott, *Aquarius Salinity Retrieval Algorithm Theoretical Basis Document (ATBD), Addendum 3*. Santa Rosa, CA, USA: Remote Sens. Syst., Jun. 2014. [Online]. Available: http://podaac.jpl.nasa.gov/SeaSurfaceSalinity/Aquarius

[5] T. Meissner, F. Wentz, D. Le Vine, and P. De Mattheis, *Aquarius Salinity Retrieval Algorithm Theoretical Basis Document (ATBD), Addendum 4*. Santa Rosa, CA, USA: Remote Sens. Syst., Jul. 2015. [Online]. Available: http://podaac.jpl.nasa.gov/SeaSurfaceSalinity/Aquarius

[6] T. Meissner, F. Wentz, and L. Ricciardulli, "The emission and scattering of L-band microwave radiation from rough ocean surfaces and wind speed measurements from Aquarius," *J. Geophys. Res. Oceans*, vol. 119, no. 9, pp. 6499–6522, Sep. 2014, doi: 10.1002/2014JC009837.

[7] D. M. Le Vine *et al.*, "Status of Aquarius/SAC-D and Aquarius Salinity Retrievals," *IEEE J. Sel. Top. Appl. Earth Observ. Remote Sens.*, vol. 8, no. 12, pp. 5401–5415, Dec. 2015, doi: 10.1109/JSTARS.2015.2427159.

[8] G. Lagerloef and H. Y. Kao, Aquarius Salinity Validation Analysis; Data Version 4.0. Earth Space Res., Seattle, WA, USA, Aug. 2015. [Online]. Available: http://podaac.jpl.nasa.gov/SeaSurfaceSalinity/Aquarius

[9] S. Misra and C. Ruf, "Detection of radio-frequency interference for the Aquarius radiometer," *IEEE Trans. Geosci. Remote Sens.*, vol. 46, no. 10, pp. 3123–3128, Oct. 2008, doi: 10.1109/TGRS.2008.920371.

[10] T. Meissner, F. Wentz, L. Ricciardulli, K. Hilburn, and J. Scott, "The aquarius salinity retrieval algorithm: Recent progress and remaining challenges," *Proc. 13th Spec. Meet. Microw. Radiometry Remote Sens. Environ.*, Pasadena, CA, USA, Mar. 24–27, 2014, pp. 49–54, doi: 10.1109/MicroRad.2014.6878906.

[11] T. Meissner and F. Wentz, "The complex dielectric constant of pure and sea water from microwave satellite observations," *IEEE Trans. Geosci. Remote Sens.*, vol. 42, no. 9, pp. 1836–1849, Sep. 2004.

[12] T. Meissner and F. Wentz, "The emissivity of the ocean surface between 6–90 GHz over a large range of wind speeds and earth incidence angles," *IEEE Trans. Geosci. Remote Sens.*, vol. 50, no. 8, pp. 3004–3026, Aug. 2012.

[13] "Aquarius official release level 2 sea surface salinity. Ver. 4.0," NASA Aquarius project, PO.DAAC, Pasadena, CA, USA, 2015. [Online]. Available: http://dx.DOI.org/10.5067/AQR40-2SOCS

[14] R. W. Reynolds and T. M. Smith, "Improved global sea surface temperature analyses using optimum interpolation," *J. Clim.*, vol. 7, no. 6, pp. 929–948, Jun. 1994, doi: 10.1175/1520-0442(1994)0072.0.CO;2.

[15] R. W. Reynolds, T. M. Smith, C. Liu, D. B. Chelton, K. S. Casey, and M. G. Schlax, "Daily high-resolution blended analyses for sea surface temperature," *J. Climate*, vol. 20, no. 22, pp. 5473–5496, 2007, doi: 10.1175/JCLI-D-14-00293.1.

[16] *The NOAA Optimum Interpolation 1/4 Degree Daily Sea Surface Temperature Analysis (OISST): AVHRR-Only*. [Online]. Available: http://www.ncdc.noaa.gov/oisst

[17] F. J. Wentz, L. Ricciardulli, C. Gentemann, T. Meissner, K. A. Hilburn, and J. Scott, *Remote Sensing Systems Coriolis WindSat Daily. Environmental Suite on 0.25 deg grid, Version 7.0.1, Sea Surface Temperature*. Santa Rosa, CA, USA: Remote Sens. Syst., 2013. [Online]. Available: www.remss.com/missions/windsat

[18] B. Brasnett, "The impact of satellite retrievals in a global sea-surface-temperature analysis," *Q. J. R. Meteorol. Soc.*, vol. 134, no. 636, pp. 1745–1760, 2008, doi: 10.1002/qj.319.

[19] T. M. Chin, J. Vazquez, and E. Armstrong, "Algorithm theoretical basis document: A multi-scale, high-resolution analysis of global sea surface temperature, version 1.3," NASA Jet Propulsion Lab., Pasadena, CA, USA, Jun. 2013. [Online]. Available: ftp://mariana.jpl.nasa.gov/mur_sst/tmchin/docs/ATBD/

[20] C. L. Gentemann, P. J. Minnett, and B. Ward, "Profiles of Ocean Surface Heating (POSH): A new model of upper ocean diurnal warming," *J. Geophys. Res. Oceans*, vol. 114, no. C7, 2009, Art. no. C07017, doi: 10.1029/2008JC004825.

[21] Hybrid Coordinate Ocean Model, GLBa0.08/expt_90.9, Top Layer Salinity. [Online]. Available: www.hycom.org

[22] J. A. Cummings and O. M. Smedstad, "Variational data assimilation for the global ocean. Data assimilation for atmospheric," in *Oceanic and Hydrologic Applications*, vol. 2. Berlin, Germany: Springer-Verlag, 2013, ch. 13, pp. 303–343, doi: 10.1007/978-3-642-35088-7_13.

[23] J. A. Cummings, "Operational multivariate ocean data assimilation," *Quart. J. Roy. Meteorol. Soc. C*, vol. 131, no. 613, pp. 3583–3604, Oct. 2005, doi: 10.1256/qj.05.105.

[24] D. N. Fox, W. J. Teague, C. N. Barron, M. R. Carnes, and C. M. Lee, "The Modular Ocean Data Assimilation System (MODAS)," *J. Atmos. Ocean. Technol.*, vol. 19, pp. 240–252, 2002.

[25] Asia-Pacific Data-Research Center (APDRC), *Monthly 3° × 3° Averaged ARGO Salinity Fields at 0 m*. [Online]. Available: http://apdrc.soest.hawaii.edu/projects/Argo/

[26] J. Font, G. Lagerloef, D. Le Vine, A. Camps, and O. Zanife, "The determination of surface salinity with the European SMOS space mission," *IEEE Trans. Geosci. Remote Sens.*, vol. 42, no. 10, pp. 2196–2205, Oct. 2004, doi: 10.1109/TGRS.2004.834649.

[27] D. E. Entekhabi *et al.*, "The Soil Moisture Active Passive (SMAP) mission," *Proc. IEEE*, vol. 98, no. 5, pp. 704–716, May 2010, doi: 10.1109/JPROC.2010.2043918.

[28] T. Meissner, F. J. Wentz, and J. Scott, *Remote Sensing Systems SMAP 8 Day and Monthly Mean Sea Surface Salinity on 0.25 deg Grid, Version 1.0. (BETA)*. Santa Rosa, CA, USA: Remote Sens. Syst., 2015. [Online]. Available: www.remss.com/missions/smap

Thomas Meissner (M'02–SM'13) was born in Germany and received the B.S. degree in physics from the University of Erlangen-Nürnberg, Erlangen, Germany, in 1983, the M.S. (Diploma) degree in physics from the University of Bonn, Bonn, Germany, in 1987, and the Ph.D. degree in theoretical physics from the Ruhr-Universitäät Bochum, Bochum, Germany, in 1991, writing his doctoral dissertation on effective quark models of the nucleon.

Between 1992 and 1998, he conducted postdoctoral research with the University of Washington, Seattle, WA, USA; the University of South Carolina, Columbia, SC, USA; and at Carnegie Mellon University, Pittsburgh, PA, USA, in theoretical nuclear and particle physics focusing on the theory of strong interaction. In July 1998, he joined Remote Sensing Systems (RSS), Santa Rosa, CA, USA. Since then, he has been working on the development and refinement of radiative transfer models, calibration, validation, and ocean retrieval algorithms for various microwave instruments (Special Sensor Microwave Imager (SSM/I), Tropical Rainfall Measuring Mission microwave imager, Advanced Microwave Scanning Radiometer onboard the Earth Observing Satellite, WindSat, Conical Microwave Imager Sounder (CMIS), Special Sensor Microwave Imager Sounder (SSMIS), Global Precipitation Measurement Microwave Imager (GMI), Aquarius, Soil Moisture Active Passive).

Dr. Meissner is a member of the American Physical Society, the American Geophysical Union, and the American Meteorological Society. As a member of the Aquarius Launch, Early Orbit Operations, and Commissioning Team, he has been recognized with the NASA Group Achievement Award in 2012. In 2013, he and Frank Wentz were recipients of the IEEE TRANSACTIONS ON GEOSCIENCE AND REMOTE SENSING Prized Paper Award for the paper describing the RSS ocean radiative transfer model. He has been serving on the review panel for the National Academy of Sciences Committee on Radio Frequencies.

Frank J. Wentz received the B.S. and M.S. degrees in physics from the Massachusetts Institute of Technology, Cambridge, MA, USA, in 1969 and 1971, respectively.

In 1974, he founded Remote Sensing Systems (RSS), a research company specializing in satellite microwave remote sensing of the Earth. As a member of the NASA's SeaSat Experiment Team (1978–1982), he pioneered the development of physically based retrieval methods for microwave scatterometers and radiometers. Starting in 1987, he took the lead in providing the research community with high-quality ocean products derived from satellite microwave imagers. In 1998, he discovered a flaw (neglect of orbit decay) in the existing satellite air temperature record, which, at that time, was showing no warming. When properly processed, the satellite time series exhibited a warming trend consistent with the satellite observations of atmospheric water and also with the surface temperature measurements. He has played a key role in demonstrating the capability for microwave remote sensing to measure the temperature of the world's oceans through clouds. More recently, he has been using satellite measurements to study the impact that surface winds, evaporation, and precipitation have on the acceleration of the hydrologic cycle. As the Director of RSS, he oversees the production and validation of research-quality satellite climate products. These RSS products are freely provided to the Earth science community. His research interests include the physics of microwave emission and scattering from rough ocean surfaces.

Mr. Wentz is an Elected Fellow of the American Geophysical Union, the American Meteorological Society (AMS), and the American Association for the Advancement of Science. In 2013, he and Dr. T. Meissner were the recipients of the IEEE TRANSACTIONS ON GEOSCIENCE AND REMOTE SENSING Prized Paper Award for the paper describing the RSS ocean radiative transfer model. In 2015, he was the recipient of the Verner E. Suomi Award for satellite meteorology from the AMS.

Joel Scott received the M.S. degree in atmospheric science from Florida State University, Tallahassee, FL, USA, with a focus in remote sensing applied to air–sea interaction and boundary-layer processes and the B.S. degree in meteorology and mathematics (*summa cum laude*) from Texas A&M University, College Station, TX, USA.

He joined Remote Sensing Systems (RSS) in 2011, where he has worked with active and passive satellite microwave instruments, including SSM/I, SSMIS, Tropical Rainfall Measuring Mission microwave imager, WindSat, Advanced Microwave Scanning Radiometer onboard the Earth Observing Satellite, Advanced Microwave Scanning Radiometer 2 (AMSR2), GMI, Aquarius SAC-D (L-band radiometer, scatterometer, and Microwave Radiometer (MWR)), and Soil Moisture Active Passive. His research interest includes designing and generating a storm-centric database for studying tropical cyclones' cold wakes and has been largely responsible for porting and updating the CCMP V2.0 vector wind analysis product source code, which is operationally running at RSS. In April 2016, he has been with the Ocean Biology Processing Group, NASA Goddard Space Flight Center.

Jorge Vazquez-Cuervo received the B.S. degree in physics (with honors) from the University of Miami, Coral Gables, FL, USA, in 1980, the M.S. degree in physical oceanography from the Graduate School of Oceanography, University of Rhode Island, Kingston, RI, USA, in 1984, and the Ph.D. degree in geological sciences from the University of Southern California, Los Angeles, CA, USA, in 1992.

He started his research working with sea-level data from the Geodetic/Geophysical Satellite (GEOSAT) altimeter focusing on the meandering of the Gulf Stream. He was a Visiting Scientist with the Instituto de Ciencias del Mar, Barcelona, Spain. There, he focused on using altimetry data to study the space and timescales of the Alboran Gyres. Since 1993, he has been with the Jet Propulsion Laboratory, California Institute of Technology, Pasadena, CA. His research has focused on the use of sea surface temperature data. He has been also instrumental in the development and coordination of the Group for High Resolution Sea Surface Temperature. Currently, he serves as the Project Science Team lead for sea surface temperature and salinity for NASA's Physical Oceanography Distributed Active Archive Center (PO.DAAC).